

# Vertical Single-Walled Carbon Nanotube Arrays via Block Copolymer Lithography

Duck Hyun Lee, Won Jong Lee,\* and Sang Ouk Kim\*

Department of Materials Science and Engineering, KAIST 373-1, Guseong-dong, Yuseong-gu, Daejeon 305-701, Republic of Korea

Received December 22, 2008. Revised Manuscript Received January 31, 2009

The growth of vertical single-walled carbon nanotube (SWNT) arrays of uniform aerial distribution is achieved by oxygen assisted plasma enhanced chemical vapor deposition (PECVD) growth from nanopatterned catalyst arrays prepared by block copolymer lithography. Block copolymer lithography is an attractive nanopatterning method for generating a uniform catalyst particle array for carbon nanotube growth. Nevertheless, the scale of the catalyst particles patterned by block copolymer lithography is usually not small enough for SWNT growth. In this work, various methods to reduce the catalyst size have been investigated for SWNT growth. Nanopatterned iron catalyst arrays having a mean diameter of 9 nm were prepared via tilted evaporation of thin iron catalyst films over a block copolymer template with the nanopore size of 20 nm, followed by heat treatment at 600 °C. The catalyst particle size was further reduced to the size required for SWNT growth (~3 nm) by the following two methods. In method i, the catalyst particles were sequentially annealed at 800 °C first in air and then in an H<sub>2</sub> atmosphere. The evaporation of iron atoms and subsequent reduction during heat treatment produced catalyst particles sufficiently small for SWNT growth. In method ii, an Al layer was deposited over the catalyst array, which decreased the exposed area of the catalyst particles. The effective catalyst particle size was thus reduced, which enabled the growth of SWNTs.

## Introduction

Densely grown vertical single-walled carbon nanotube (SWNT) arrays possess many appealing properties useful for applications ranging from electronics to energy storage devices.<sup>1–4</sup> However, selective growth of SWNTs of uniform aerial distribution is a principal and challenging issue.<sup>5,6</sup> A key breakthrough is the growth of SWNT arrays by chemical vapor deposition (CVD) from uniformly distributed small catalyst particles, since the size, aerial density, and location of the carbon nanotubes (CNTs) are all determined by the size and spatial distribution of catalyst particles. One common method of preparing catalyst particles is the deposition of thin catalyst films on substrates. Subsequent thermal annealing at elevated temperature leads to the formation of randomly distributed polydisperse catalyst nanoparticles.<sup>7–9</sup> However, this method does not allow for precise control of catalyst size, spacing, or location. An alternative approach to prepare uniform catalyst particle

arrays is nanopatterning catalyst particles using block copolymer lithography.<sup>5,6,10–15</sup>

Block copolymers, self-assembling materials consisting of two or more covalently linked chemically distinct polymer blocks, may provide a variety of periodic nanoscale morphologies having feature sizes ranging from 5 to 50 nm.<sup>16,17</sup> Owing to the diverse pattern shapes and fine-tunability of their pattern sizes, block copolymer nanostructures have been widely used as templates for nanoscale lithography.<sup>18–28</sup> Recently, considerable efforts have been devoted to the preparation of nanopatterned metal catalyst arrays for CNT and nanowire growth by block copolymer lithography. Nevertheless, the scale of the patterned catalyst nanoparticles is usually not small enough for the growth of SWNTs.<sup>10–15</sup>

\* Corresponding authors. E-mail: wjlee@kaist.ac.kr (W.J.L.), sangouk.kim@kaist.ac.kr (S.O.K.). Office phone: +82-42-350-3339 (S.O.K.). Fax: +82-42-350-3310 (S.O.K.).

- (1) Terrones, M. *Int. Mater. Rev.* **2004**, *49*, 325.
- (2) Baughman, R. H.; Zakhidov, A. A.; de Heer, W. A. *Science* **2002**, *297*, 787.
- (3) Sekitani, T.; Noguchi, Y.; Hata, K.; Fukushima, T.; Aida, T.; Someya, T. A. *Science* **2008**, *321*, 1468.
- (4) Cao, Q.; Kim, H. S.; Pimparkar, N.; Kulkarni, J. P.; Wang, C.; Shim, M.; Roy, K.; Alam, M. A.; Rogers, J. A. *Nature* **2008**, *454*, 495.
- (5) Lastella, S.; Jung, Y. J.; Yang, H.; Vajtai, R.; Ajayan, P. M.; Ryu, C. Y.; Rider, D. A.; Manners, I. *J. Mater. Chem.* **2004**, *14*, 1791.
- (6) Lu, J. Q.; Kopley, T. E.; Moll, N.; Roitman, D.; Chamberlin, D.; Fu, Q.; Liu, J.; Russell, T. P.; Rider, D. A.; Manners, I.; Winnik, M. A. *Chem. Mater.* **2005**, *17*, 2227.

- (7) Murakami, Y.; Chiashi, S.; Miyauchi, Y.; Hu, M.; Ogura, M.; Okubo, T.; Maruyama, S. *Chem. Phys. Lett.* **2004**, *385*, 298.
- (8) Hata, K.; Futaba, D. N.; Mizuno, K.; Namai, T.; Yumura, M.; Iijima, S. *Science* **2004**, *306*, 1362.
- (9) Zhong, G.; Iwasaki, T.; Honda, K.; Furukawa, Y.; Ohdomari, I.; Kawarada, H. *Jpn. J. Appl. Phys.* **2005**, *44*, 1558.
- (10) Bennett, R. D.; Xiong, G. Y.; Ren, Z. F.; Cohen, R. E. *Chem. Mater.* **2004**, *16*, 5589.
- (11) Bennett, R. D.; Hart, A. J.; Cohen, R. E. *Adv. Mater.* **2006**, *18*, 2274.
- (12) Liu, X.; Bigioni, T. P.; Xu, Y.; Cassell, A. M.; Cruden, B. A. *J. Phys. Chem. B* **2006**, *110*, 20102.
- (13) Lu, J. Q. *J. Phys. Chem. C* **2008**, *112*, 10344.
- (14) Lee, D. H.; Shin, D. O.; Lee, W. J.; Kim, S. O. *Adv. Mater.* **2008**, *20*, 2480.
- (15) Lee, D. H.; Shin, D. O.; Lee, W. J.; Kim, S. O. *J. Nanosci. Nanotech.* **2008**, *8*, 5571.
- (16) Hamley, I. W. *Developments in block copolymer science and technology*; Wiley: New York, 2004.
- (17) Bates, F. S.; Fredrickson, G. H. *Annu. Rev. Phys. Chem.* **1990**, *41*, 525.

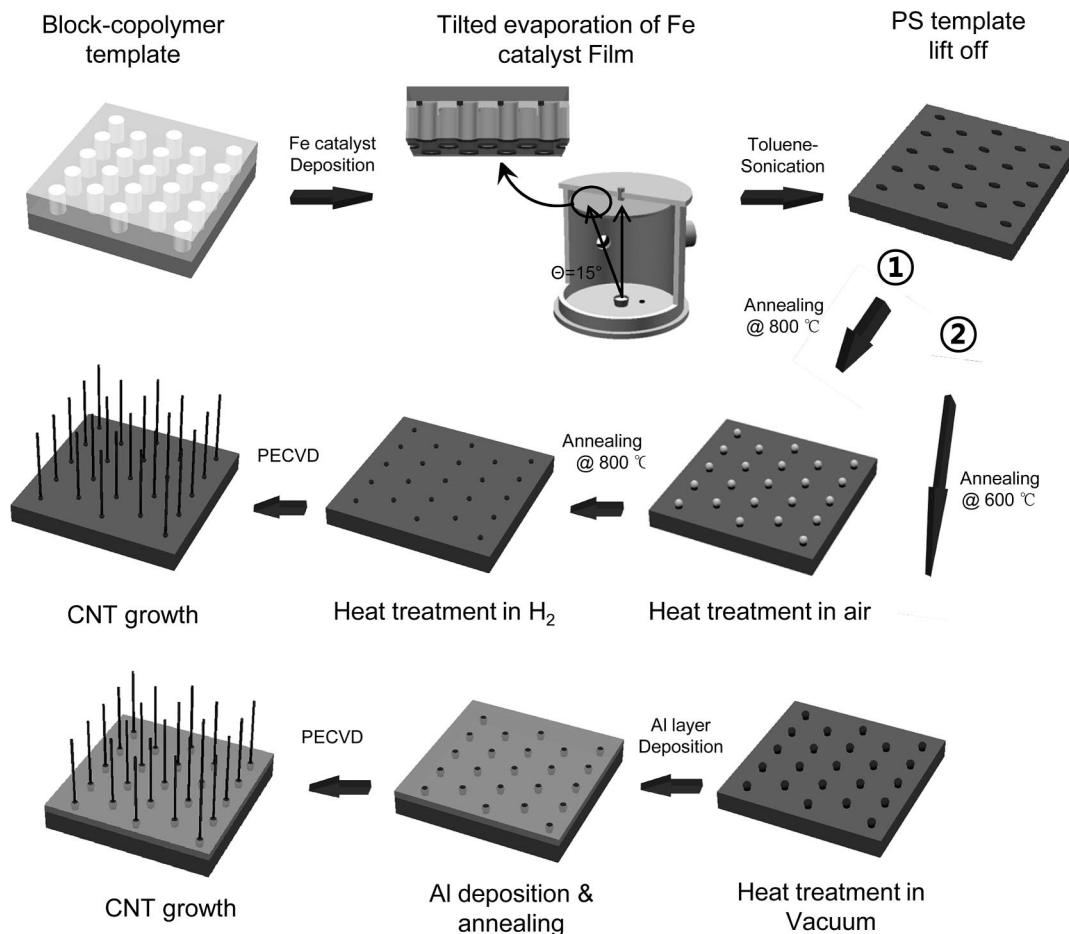


**Figure 1.** Schematic diagram of the synthetic processes for vertical SWNT arrays.

In this work, we introduce two approaches for growing vertical SWNT arrays from the catalyst array prepared by block copolymer lithography. Self-assembled thin films of asymmetric block copolymers, polystyrene-block-poly-(methyl methacrylate)s (PS-*b*-PMMA), provided hexagonal nanoporous PS templates (pore diameter 20 nm, center-to-center distance between neighboring pores 35 nm) over a large area. The pore size of the block copolymer nanotemplate was relatively large for the formation of  $\sim 2$  nm catalyst particles, which is required for the growth of SWNT arrays. Tilted evaporation (tilting angle  $15^\circ$ ) of an iron layer over the PS template created nanopatterned iron catalysts (diameter  $\sim 9$  nm) smaller than the pore size of the block copolymer template. Subsequent processes (method i sequential heat treatment in air and  $H_2$  or method ii embedding the catalyst array in an Al layer) allowed for the formation of iron catalyst arrays small enough to grow SWNT arrays.

## Experimental Section

**Materials.** An asymmetric block copolymer, PS-*b*-PMMA forming cylindrical nanostructures (molecular weight PS/PMMA 46 000/21 000) was purchased from Polymer Source Inc. The iron source for E-beam evaporation (purity 99.95%) was purchased from Thifine. Pure oxygen, hydrogen, and acetylene gas was purchased from Kyungin Chemical Industrial.

**Nanopatterned Catalyst Particle Preparation.** A schematic diagram outlining the entire process for growing vertical SWNT arrays is presented in Figure 1. A silicon wafer surface was neutrally treated with a random copolymer brush.<sup>29,30</sup> A thin film (film thickness 42 nm) of cylindrical block copolymer was spin-coated onto the wafer surface. High temperature annealing at  $190^\circ\text{C}$  generated a self-assembled block copolymer thin film that consisted of a PMMA cylinder array perpendicular to the substrate surface

- (18) Kim, D. H.; Kim, S. H.; Lavery, K.; Russell, T. P. *Nano Lett.* **2004**, *4*, 1841.
- (19) Nagarajan, S.; Li, M.; Pai, R. A.; Bosworth, J. K.; Busch, P.; Smilgies, D.-M.; Ober, C. K.; Russell, T. P.; Watkins, J. J. *Adv. Mater.* **2008**, *20*, 246.
- (20) Park, M.; Harrison, C.; Chaikin, P. M.; Register, R. A.; Adamson, D. H. *Science* **1997**, *276*, 1401.
- (21) Thurn-Albrecht, T.; Schotter, J.; Kastle, G. A.; Emley, N.; Shibauchi, T.; Krusin-Elbaum, L.; Guarini, K.; Black, C. T.; Tuominen, M. T.; Russell, T. P. *Science* **2000**, *290*, 2126.
- (22) Kim, S. O.; Solak, H. H.; Stoykovich, M. P.; Ferrier, N. J.; dePablo, J. J.; Nealey, P. F. *Nature* **2003**, *424*, 411.

- (23) Stoykovich, M. P.; Muller, M.; Kim, S. O.; Solak, H. H.; Edwards, E. W.; de Pablo, J. J.; Nealey, P. F. *Science* **2005**, *308*, 1442.
- (24) Bita, I.; Yang, J. K. W.; Jung, Y. S.; Ross, C. A.; Thomas, E. L.; Berggren, K. K. *Science* **2008**, *321*, 939.
- (25) Ruiz, R.; Kang, H.; Detcheverry, F. A.; Dobisz, E.; Kercher, D. S.; Albrecht, T. R.; de Pablo, J. J.; Nealey, P. F. *Science* **2008**, *321*, 936.
- (26) Tang, C.; Lennon, E. M.; Fredrickson, G. H.; Kramer, E. J.; Hawker, C. J. *Science* **2008**, *322*, 429.
- (27) Kim, S. O.; Kim, B. H.; Meng, D.; Shin, D. O.; Koo, C. M.; Solak, H. H.; Wang, Q. *Adv. Mater.* **2007**, *19*, 3271.
- (28) Kim, B. H.; Shin, D. O.; Jeong, S. J.; Koo, C. M.; Jeon, S. C.; Hwang, W. J.; Lee, S.; Lee, M. G.; Kim, S. O. *Adv. Mater.* **2008**, *20*, 2303.
- (29) Mansky, P.; Liu, Y.; Huang, E.; Russell, T. P.; Hawker, C. *Science* **1997**, *275*, 1458.
- (30) Jeong, S. J.; Xia, G.; Kim, B. H.; Shin, D. O.; Kwon, S. H.; Kang, S. W.; Kim, S. O. *Adv. Mater.* **2008**, *20*, 1898.

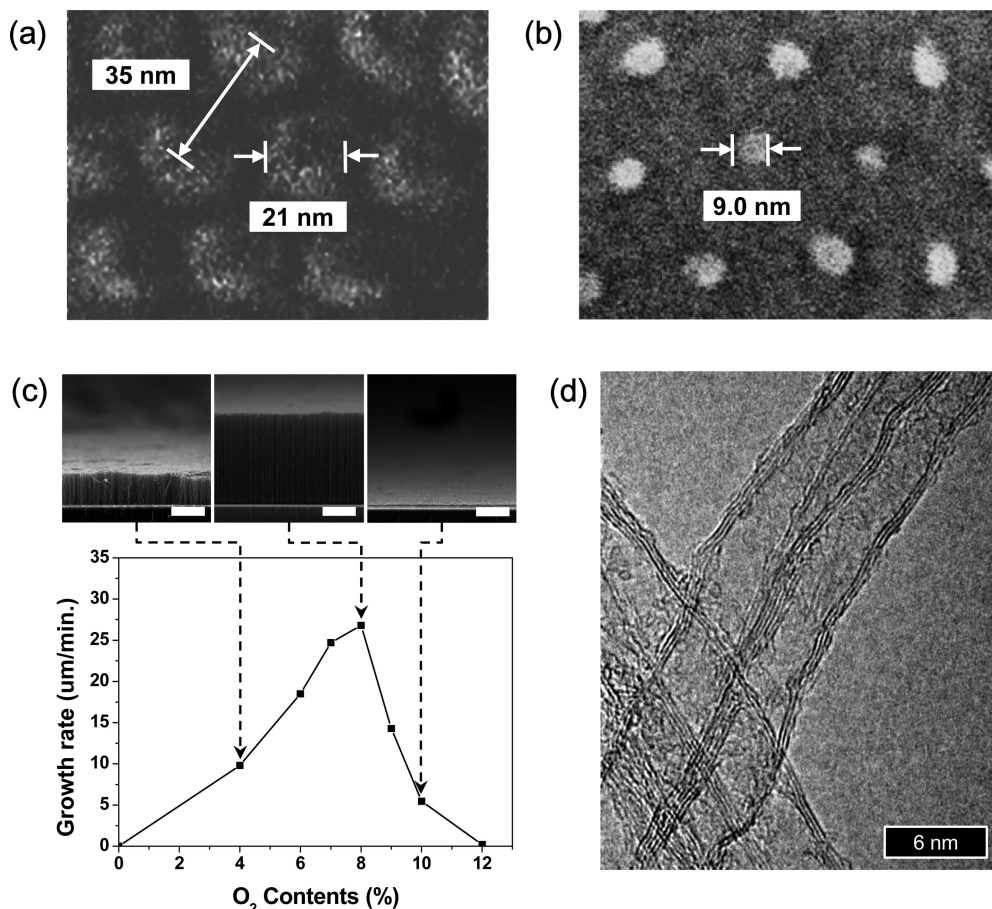


**Figure 2.** High-magnification SEM images of the nanopatterned iron catalyst particles prepared by tilted deposition through a block copolymer nanotemplate (tilting angle 15°, evaporation thickness 0.7 nm) (a) before and (b) after heat treatment at 600 °C. (c) CNT growth rate plotted as a function of environmental gas O<sub>2</sub> content. The environmental and feed gas flow rates were fixed at 100 and 25 sccm, respectively. (inset) Cross-sectional SEM images, presented at the same magnification, comparing the heights of CNT arrays grown at various O<sub>2</sub> contents for 1 min. The scale bar is 10 μm. (d) High-resolution TEM (HRTEM) images of multiwalled CNTs (MWNTs) grown from the catalyst array prepared by tilted deposition through a block copolymer nanotemplate.

in a PS matrix. The self-assembled block copolymer thin film was exposed to UV radiation and subsequently rinsed with acetic acid to remove the PMMA cylinder cores leaving a cross-linked nanoporous PS template intact. An iron catalyst film (film thickness 0.7 nm) was deposited over the block copolymer template via tilted evaporation at 15°. After deposition, the remaining PS nanoporous template was lifted off by sonication in toluene. In method i, the patterned iron catalyst particles were sequentially heat treated at 800 °C in air for up to 30 min and in a H<sub>2</sub> environment for up to 20 min. In method ii, the patterned iron catalyst particles were heat treated at 600 °C. This resulted in 9 nm diameter spherical catalyst particles. An Al layer was then deposited with a thickness of up to 10 nm by thermal evaporation and heat treated at 700 °C.

**CVD Growth of Vertical CNTs.** CNTs were grown on the catalyst-deposited substrates by the plasma enhanced chemical vapor deposition (PECVD) method. The substrate was heated to 600 °C under a mixture of H<sub>2</sub> and O<sub>2</sub> gas flow (chamber pressure 0.4 torr). The O<sub>2</sub> content varied between 0 and 12 vol %, and the total flow of the environmental gas was fixed as 100 sccm. The chamber pressure was then increased to 5 torr, and direct current (DC) plasma was activated via an anode DC voltage of 470 V relative to the grounded substrate. Slow streaming of the acetylene source gas at a flow rate of 25 sccm for 1 min led to dense vertical carbon nanotube arrays grown from the patterned iron catalyst arrays.

**Measurement of CNT Wall Number.** CNT wall number was measured using transmission electron microscopy (TEM). The sample preparation procedure was as follows. The as-grown CNTs

were ultrasonically detached from the substrate and dispersed in ethanol. A drop of the CNT dispersion was deposited onto a carbon-supported TEM grid and air-dried. For statistical analyses, the wall number of 100 randomly chosen CNTs was measured from the TEM images.

## Results and Discussion

There are two decisive factors governing the growth of vertical SWNT arrays.<sup>31</sup> First, a supply of an adequate environmental gas is required. Since the accumulation of amorphous carbon at the catalyst particle surface during chemical vapor deposition (CVD) processes severely degrades the activity and lifetime of those particles, selection of an adequate environmental gas that can selectively remove amorphous carbon without damaging CNTs is crucial. Second, preparation of sufficiently small catalyst particles and prevention of agglomeration of those particles is highly significant.

Scanning electron microscopy (SEM) images of hexagonally packed iron particles show the as-deposited iron particles to be anisotropic (Figure 2a). This anisotropy results from tilted deposition through a block copolymer nanotem-

(31) Kayastha, V. K.; Wu, S.; Moscatello, J.; Yap, Y. K. *J. Phys. Chem. C* **2007**, *111*, 10158.



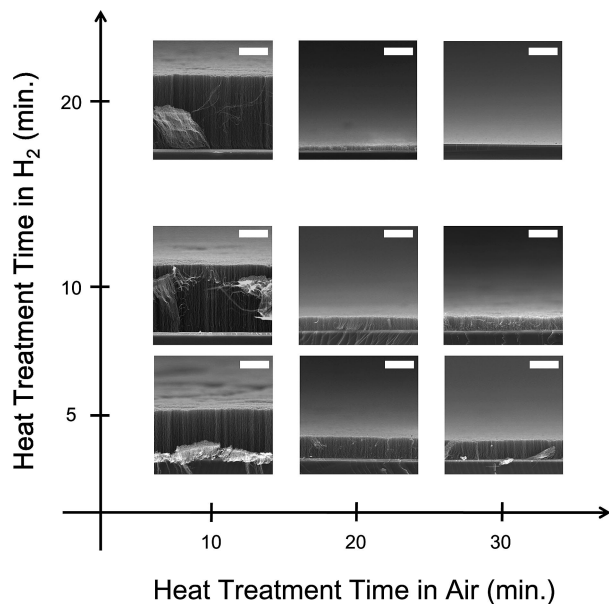


**Figure 3.** Cross-sectional SEM images of the grown CNT arrays plotted as a function of sequential heat treatment time in air and  $H_2$ .

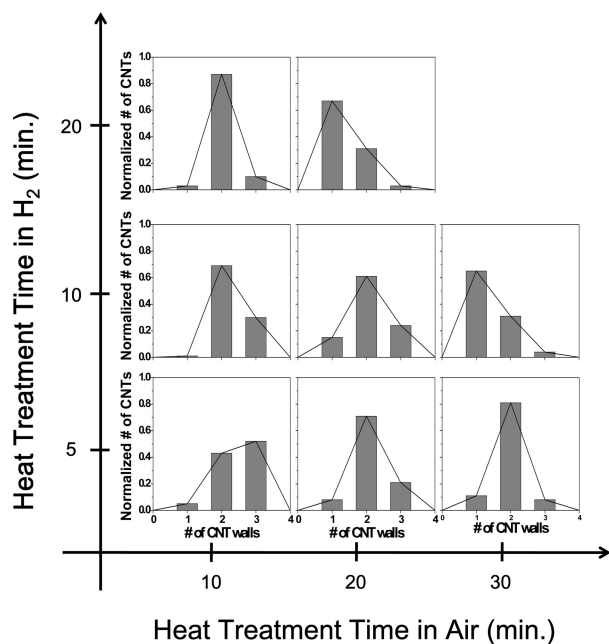


**Figure 4.** Statistical wall number distribution of CNTs plotted as a function of sequential heat treatment time in air and  $H_2$ .

plate (tilting angle  $15^\circ$ , thickness 0.7 nm). After heat treatment at  $600^\circ\text{C}$  in vacuum, the catalyst particles agglomerated to become isotropic with a reduced diameter of 9 nm (Figure 2b). The size of the agglomerated catalyst particles was highly monodisperse over the substrate size of  $1 \times 1 \text{ cm}^2$ .

For optimizing CNT growth conditions, the CNT growth rate was investigated as a function of the  $O_2$  content in the environmental gas (Figure 2c). The growth temperature of  $600^\circ\text{C}$  and environmental gas flow rate of 100 sccm were fixed for all compositions. As oxygen plasma is a strong etching gas for carbon, the growth rate of CNT arrays is strongly dependent on the  $O_2$  content in the environmental

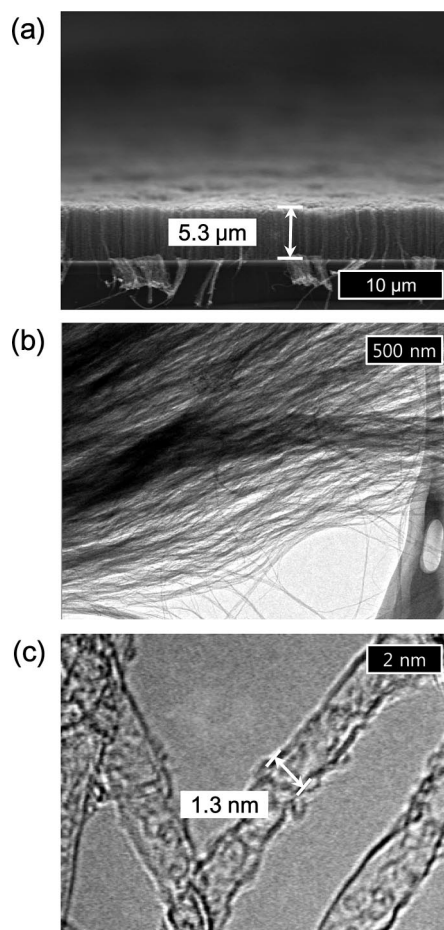


**Figure 5.** (a) Cross-sectional SEM and (b and c) TEM images of the SWNT arrays grown from the catalyst array prepared by method i (sequentially heat treated at  $800^\circ\text{C}$  in air for 30 min and in an  $H_2$  atmosphere for 10 min).

gas. The inset SEM images compare the vertical CNT arrays grown at various  $O_2$  content values, and they clearly demonstrate the variation of growth rate with  $O_2$  content. As oxygen plasma effectively removes amorphous carbon contaminant at the surface of catalyst particles, the growth rate of CNT arrays increased with increasing  $O_2$  content up to 8%. However, further increase in  $O_2$  content led to a decrease in the CNT array growth rate, which was due to the etching of growing CNTs by oxygen plasma. An  $O_2$  content of 8% provided the highest growth rate at  $27 \mu\text{m}/\text{min}$ . A high-resolution transmission electron microscopy (HRTEM) image of the CNT arrays grown from catalyst particles having an average diameter of 9 nm is shown in Figure 2d. The CNT arrays had an average diameter of 6 nm, and the majority (70%) of them were triple-walled.

For SWNT growth, the size of catalyst particles was further reduced by two methods. In method i, the patterned catalyst particles were sequentially heat treated first in air and then in an  $H_2$  atmosphere. The patterned catalyst array was placed in a furnace, and the environmental temperature was gradually raised at a rate of  $40^\circ\text{C}/\text{min}$ . At first, the patterned catalyst particles were heat treated in air at  $800^\circ\text{C}$  for up to 30 min. The small size and high surface area of

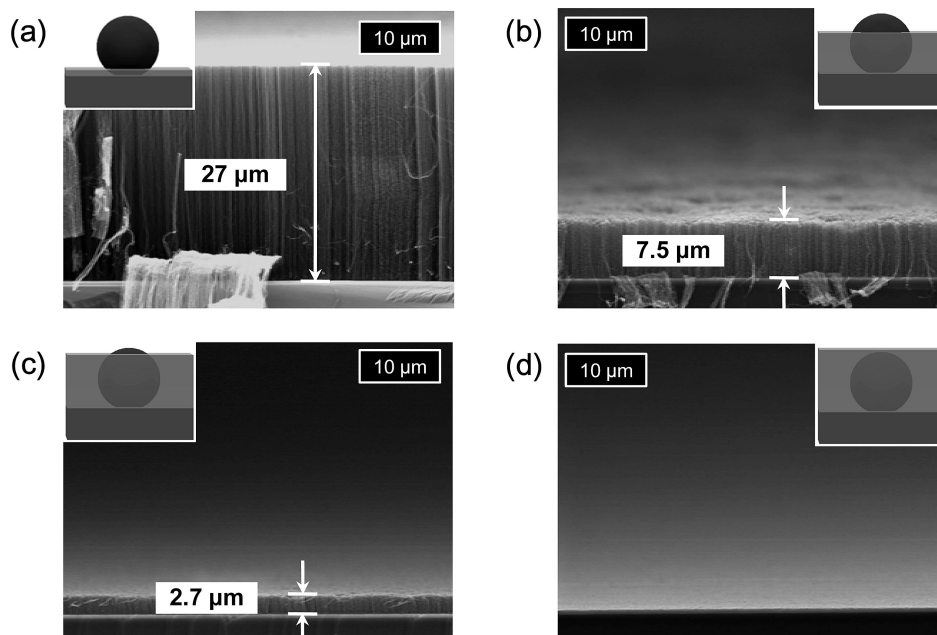


**Figure 6.** Cross-sectional SEM images of the CNT arrays grown on the catalyst particles embedded in Al layers of thicknesses (a) 2, (b) 7, (c) 9, and (d) 10 nm. The inset images are schematic diagrams of the catalyst particles embedded in the Al layer.

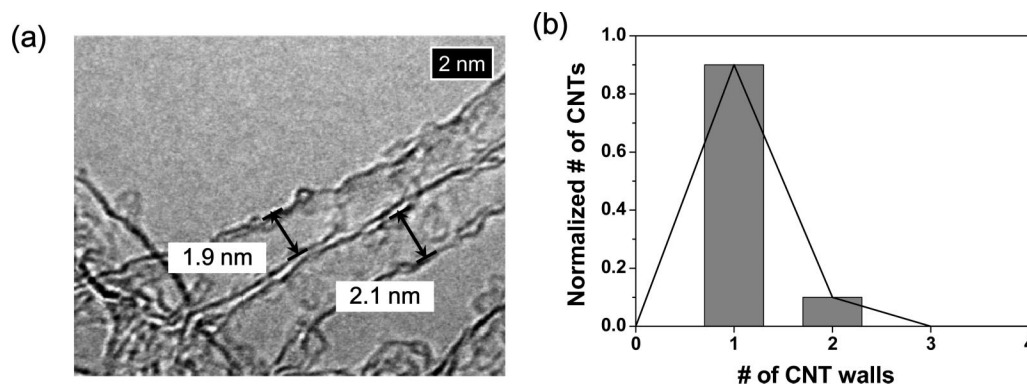


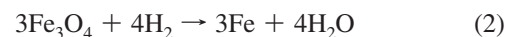
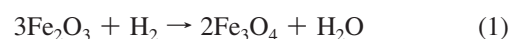
**Figure 7.** (a) HRTEM image and (b) statistical wall number distribution of the vertical SWNT arrays grown from the catalyst array embedded in the Al layer with a thickness of 9 nm.

catalyst particles result in a high activity and decreased phase transition energy.<sup>32</sup> According to the following Kelvin equation:

$$RT \ln\left(\frac{P}{P_0}\right) = \frac{2\gamma V_m}{r}$$

where  $P$  is the actual vapor pressure,  $P_0$  is the saturated vapor pressure,  $\gamma$  is the surface tension,  $V_m$  is molar volume,  $R$  is the universal gas constant,  $r$  is the radius of the particle, and  $T$  is temperature. The saturated vapor pressure of small particles generally is higher than that of the bulk material. For iron nanoparticles, the saturated vapor pressure is several times higher than that of bulk iron. Due to this elevated vapor pressure, when iron nanoparticles were heat treated at 800 °C, iron atoms rapidly evaporated from its (the nanoparticle's) surface, which decreases the particle size. The quantity of evaporated iron was roughly proportional to the heat treatment time.<sup>30</sup> After heat treatment in air, the catalyst nanoparticles were again heat treated in a  $H_2$  environment

at 800 °C to reduce the oxidized catalyst particles. The reduction of iron oxide proceeds through the following reactions, 1 and 2.<sup>33–35</sup>



Due to selective exclusion of the oxygen atoms, the catalyst particle size decreased further by the reduction process (Supporting Information Figure S1).

Cross-sectional scanning electron microscopy (SEM) images of the grown CNT arrays were examined as a function of sequential heat treatment time in air and  $H_2$  (Figure 3). When the catalyst particles were first treated in air for 10 min, the growth rate of CNT arrays slightly increased with

(32) Zhao, B.; Wang, Y.; Guo, H.; Wang, J.; He, Y.; Jiao, Z.; Wu, M. *Mater. Sci.-Poland* **2007**, *25*, 1143.

(33) Shimokawabe, M.; Furuichi, R.; Ishii, T. *Thermochim. Acta* **1979**, *28*, 287.

(34) Sastri, M. V. C.; Viswanath, R. P.; Viswanathan, B. *Int. J. Hydrogen Energy* **1982**, *7*, 951.

(35) Mondal, K.; Lorethova, H.; Hippo, E.; Wiltowski, T.; Lalvani, S. B. *Fuel Process. Technol.* **2004**, *86*, 33.

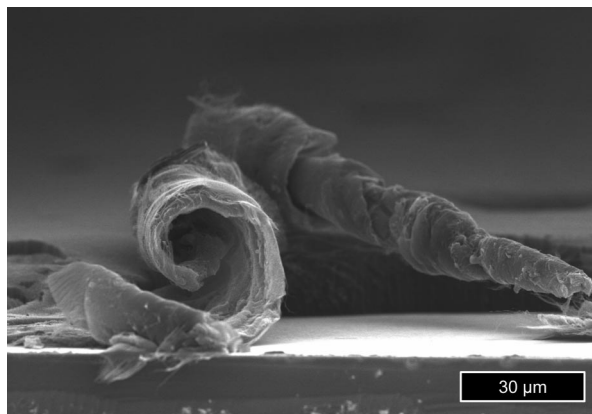


**Figure 8.** Cross-sectional SEM image of vertical SWNT arrays detached from the silicon substrate, demonstrating a high mechanical flexibility of the vertical SWNT layer.

(the subsequent)  $H_2$  treatment time. Upon  $H_2$  treatment, the catalyst particles were reduced and became more activated, which resulted in a higher growth rate of CNTs. In contrast, when the air treatment time was 20 min and above, the CNT growth rate decreased with (the subsequent)  $H_2$  treatment time. The CNT growth rate was related to the amount of carbon that was generated from the decomposition of the hydrocarbon source gas at the surface of the catalyst particles. When the air treatment time was more than 20 min, the size and surface area of the iron catalyst particles significantly decreased upon the following  $H_2$  treatment process, which resulted in the decrease of CNT growth rate. When the heat treatment time in air and  $H_2$  was 30 and 20 min, respectively, no CNT growth was observed. This indicates that the catalyst particles completely evaporated. The statistical wall number distribution was examined as a function of heat treatment time in air and  $H_2$  (Figure 4). As expected, catalyst particle size decreased with heat treatment time. The highest density of SWNT was obtained when heat treatment time in air and  $H_2$  was 30 and 10 min, respectively. Cross-sectional SEM and HRTEM images of the SWNT arrays grown in the optimized condition show the average diameter of catalyst particles to be  $\sim 3$  nm and the density of SWNT to be  $\sim 70\%$  (Figure 5).

In method ii, the effective catalyst size was reduced by the deposition of an Al film over the nanopatterned catalyst array and subsequent thermal annealing at  $700^\circ\text{C}$ . Al has a relatively low melting point ( $660^\circ\text{C}$ ), and its density ( $2.7\text{ g/cm}^3$  at  $293\text{ K}$ ) is lower than that of Fe ( $7.9\text{ g/cm}^3$  at  $293\text{ K}$ ).<sup>36,37</sup> Therefore, the heat treatment at  $700^\circ\text{C}$  melted the Al layer and caused the iron catalyst particles to sink into the Al layer. Since the cohesive energy of Al–Al bonds ( $3.39\text{ eV/atom}$ ) is lower than the cohesive energy of Fe–Fe bonds ( $4.28\text{ eV/atom}$ ),<sup>38</sup> the molten Al liquid form a concave meniscus around the Fe nanoparticles without any mixing between two components. The CNT arrays can be grown by decomposition of the carbon source at the exposed iron

catalyst surface. By decreasing the exposed area of the catalyst particles by Al deposition, the effective catalyst particle size could be reduced, thus enabling SWNT growth.

Cross-sectional SEM images of the CNT arrays grown on the catalyst particles embedded in Al layers of thicknesses (a) 2, (b) 7, (c) 9, and (d) 10 nm are shown in Figure 6. Schematic illustrations of the catalyst particle and Al layer for each thickness are shown in the inset images. For an Al thickness of 2 nm, the carbon source could be deposited in most of the surface area of the catalyst particle. Thus, the resulting CNT growth rate was similar to the value obtained without the Al layer ( $27\text{ }\mu\text{m/min}$ ) and most CNTs were multiwalled (70% MWNTs). Upon increasing Al thickness, the growth rate and the average wall number of CNTs decreased. This was due to the reduced effective size of the catalyst particles (Supporting Information Figure S2). Figure 7 shows an HRTEM image (Figure 7a) and the statistical wall-number distribution of CNTs grown on catalyst particles embedded in a 9 nm Al layer (Figure 7b). The CNTs had an average diameter of 2 nm, and 90% of them were single-walled.

The SWNT arrays grown using both method i and ii can be easily detached from the silicon substrate by mechanical scratching. The cross-sectional SEM image of a vertical SWNT array detached from its silicon substrate demonstrates its high mechanical flexibility (Figure 8). Notably, SWNT arrays could be regrown from the remaining catalyst array left behind on the substrate, after the as-grown SWNT arrays had been detached. This suggests that the SWNT arrays were grown by the base growth mode and most of the iron catalyst particles having a good adhesion with silica substrate remain on the substrate surface even after mechanical scratching. Particularly, the catalyst array prepared by method ii has a remarkably strong adhesion with the substrate surface, which is reinforced by the Al layer.

## Conclusion

In summary, we have investigated the PECVD growth of vertical SWNTs from nanopatterned iron catalyst arrays prepared by block copolymer lithography. Both the supply of an adequate environmental gas and the preparation of sufficiently small catalyst particles were important factors for aiding vertical SWNT growth. The optimized environmental gas composition for SWNT growth was investigated by varying the  $O_2$  content; 8% showed the highest growth rate of  $27\text{ }\mu\text{m/min}$ . Uniform catalyst particles having a sufficiently small size for SWNT growth (diameter  $\sim 3$  nm) were prepared by tilted evaporation of a catalyst through block copolymer nanotemplates and subsequent processes (method i sequential heat treatment in air and  $H_2$  and method ii Al layer deposition over catalyst particles). The vertical SWNT arrays were grown from the prepared catalyst particles via oxygen assisted PECVD. Upon decreasing the size of catalyst particles, the growth rate and the average diameter of CNT arrays decreased. The CNT arrays grown by method ii showed higher SWNT content (90%) than those grown by method i (70%). The lower content of SWNTs in the CNT array grown by method i is due to a broader size distribution of catalyst articles. During the size reduction of

(36) Pearson, W. B. *Crystal chemistry and physics of metals and alloys*; Wiley: New York, 1972.

(37) Kittel, C. *Introduction to solid state physics*, 6th ed.; Wiley: New York, 1986.

(38) Cui, H.; Eres, G.; Howe, J. Y.; Puretzky, A.; Varela, M.; Geoghegan, D. B.; Lowndes, D. H. *Chem. Phys. Lett.* **2003**, 374, 222.

catalyst particles by a sequential heat treatment in air and H<sub>2</sub>, the size distribution of particle sizes could become enlarged. Additionally, detaching CNTs from bottom substrate and successful regrowth confirmed that the highly flexible SWNT arrays were grown by a base growth mode.

**Acknowledgment.** This work was supported by the Center for Electronic Packaging Materials (ERC) (R11-2000-085-08004-0), World Class University (WCU) program (R32-2008-000-10051-0), the Korea Science and Engineering Foundation (KOSEF) (R11-2008-058-03002-0), the National Research Laboratory Program (R0A-2008-000-20057-0), the second stage

of the Brain Korea 21 project, and the 21st Century Frontier Research Programs (Center for Nanoscale Mechatronics & Manufacturing, 08K1401-01010), funded by the Korean government (MEST).

**Supporting Information Available:** Plane-view SEM images of the prepared catalyst array plotted as a function of sequential heat treatment time in air and H<sub>2</sub> and of the CNT arrays grown on the catalyst particles embedded in Al layers of thicknesses (a) 2, (b) 7, (c) 9, and (d) 10 nm. This material is available free of charge via the Internet at <http://pubs.acs.org>.

CM8034533